Article

Effect of Coating Thickness on the Atomic Oxygen Resistance of Siloxane Coatings Synthesized by Plasma Polymerization Deposition Technique

Lin Zhao, Xuesong Leng *, Bowen Bai ⬥, Rui Zhao, Zeyun Cai ⬥, Jianchao He, Jin Li and Hongsheng Chen *

Institute of Special Environments Physical Science, Harbin Institute of Technology (Shenzhen), Shenzhen 518055, China
* Correspondence: lengxuesong@hit.edu.cn (X.L.); chenhongsheng@hit.edu.cn (H.C.)

Abstract: Atomic oxygen in the low Earth orbit (LEO) environment is highly oxidizing. Due to the high flight speed of spacecraft, the relative kinetic energy of high-flux atomic oxygen bombarding the spacecraft surface can reach up to about 5 eV. Therefore, atomic oxygen is one of the most dangerous space environment factors in LEO, which seriously affects the safe operation and service life of spacecraft in orbit. In order to meet the requirements for the high reliability and long lifetime of spacecraft, effective protection measures must be taken on their sensitive surfaces. Siloxane is a coating with an organic–inorganic hybrid structure. Compared with SiO_2 and other inorganic atomic oxygen protective coatings, it has better flexibility and is better at anti-atomic oxygen performance. In this paper, the plasma polymerization deposition technique was used to prepare large-area siloxane coatings on different substrates with different thicknesses for improving atomic oxygen resistance by optimizing the process parameters. The thickness of the coating was measured by different methods, and the results showed that the thickness distribution was consistent. By observing the surface morphology of the coating, it was uniform and compact without obvious defects, so the uniformity of large-area coating was also ideal. The adhesion and heat/humidity resistance of siloxane coatings were examined by pull-off testing and damp-heat testing, respectively. The results showed that the siloxane coatings with a thickness of about 400 nm exhibited better physical properties. At the same time, the ground simulation testing of atomic oxygen confirmed that siloxane coatings with a thickness of 418 nm presented the best performance of atomic oxygen resistance. The atomic oxygen erosion yield of siloxane coatings with a thickness of 418 nm was as low as 5.39×10^{-27} cm^3/atoms, which was three orders of magnitude lower than that of the uncoated Kapton substrate and presented a good anti-atomic oxygen performance. Meanwhile, it has also successfully passed the damp-heat test. The coating thickness is only several hundred nanometers and does not increase the weight of the spacecraft, which makes it a relatively ideal LEO atomic oxygen protection material. Furthermore, a possible mechanism was proposed to explicate the physicochemical process of atomic oxygen attacking the coating materials.

Keywords: siloxane coating; thickness; atomic oxygen resistance; erosion; Kapton

1. Introduction

LEO is an orbit 200 to 700 km above the Earth's surface and is the main orbit for satellites and space stations [1,2]. The atmospheric environment of LEO is mainly composed of N_2, O_2, Ar, He, H and atomic oxygen, among which the atomic oxygen content is the largest component of the neutral gas composition. At an orbit of 400 km, atomic oxygen accounts over 80% of the atmospheric component of the LEO environment. In LEO, there are space environment factors, including high vacuum, thermal cycling, energetic charged particles, ultraviolet, atomic oxygen, space micrometeoroids and debris [3,4], among which atomic oxygen is considered the most destructive environmental factor [5,6]. Therefore, special attention should be paid to atomic oxygen in LEO.

Atomic oxygen is produced by the photo-dissociation of oxygen molecules (O_2) under solar ultraviolet radiation (wavelength < 243 nm) in LEO [7–10]. Due to the high degree of vacuum in space (at an orbital altitude of 500 km, the vacuum degree can reach 10^{-6} Pa [11]), the free path of atomic oxygen is very large (~10^8 m), and the probability of the reassociation or formation of ozone (O_3) is small [10].

Although the density of atomic oxygen is not very large (about 10^5~10^9 cm^{-3}) and its temperature is not very high (about 1000 K~1500 K) [12], at a shuttle altitude of 200 km, the atomic oxygen density is about 10^9 atoms/cm^3, corresponding to a flux of about 10^{15} atoms/cm^2·s. So the annual cumulative atomic oxygen flux on the shuttle surface reaches ~3.1×10^{22} atoms/cm^2 [12]. The impact energy of atomic oxygen on the surface of the spacecraft is as high as 5 eV due to the high-speed flight of the spacecraft (about 8 km/s) [13–16].

The strong oxidation and high kinetic energy of atomic oxygen are the main reasons for serious effects on spacecraft. The strong oxidation of atomic oxygen allows it to react directly with surface materials, greatly enhancing the reaction probability. Moreover, the flux of an atomic oxygen beam is high enough to cause physical and chemical reactions on the surface materials of spacecraft. Due to the active chemical properties and high impact energy of atomic oxygen, when it hits the outer surface of the spacecraft, it will cause the loss of surface material quality and thickness, resulting in changes in the surface morphology. Mechanical, thermal and optical properties will also be affected to varying degrees, especially on organic materials placed on the surface of the spacecraft, which can be severely oxidized and eroded [17,18]. When atomic oxygen impinges on the surface of materials containing C, H, O, N and S elements, gaseous products such as CO, CO_2, NO, NO_2 and water vapor will be generated, resulting in material surface mass loss, morphological changes and performance degradation [17,18]. Because of its active chemical nature and high impact energy, atomic oxygen can cause severe oxidation and erosion effects upon organic materials that are placed on the surface of spacecraft, resulting in a series of problems such as the thickness reducing, strength decreasing and surface optical/electrical performance degrading of the organic materials [19,20].

Moreover, the synergistic effects of atomic oxygen, ultraviolet radiation, cold and heat alternating, high-energy particle irradiation and other space environmental factors will accelerate the erosion of the surface materials on the spacecraft, seriously affecting the lifetime of the spacecraft and safe flight [18]. As a result, atomic oxygen becomes one of the most dangerous environmental factors in LEO space. In order to satisfy the life expectancy of the spacecraft in the LEO space, the organic materials on the spacecraft surface require enough atomic oxygen resistance [21–23].

In addition, atomic oxygen oxidation products will pollute the surface of optical devices, thermal control coatings, solar arrays and other components, which will affect the normal operation of spacecraft and shorten its service life [18]. Therefore, atomic oxygen protection is one of the key issues that must be considered in the design of LEO spacecraft.

The oxides containing silicon have better protection against atomic oxygen [24–26], which also has been confirmed by The Long Duration Exposure Facility (LDEF) and Space Station Freedom (SSF) experiments [25,26]. Siloxane coating is a new type of atomic oxygen resistance coating developed in recent years [27,28], which has excellent performance of atomic oxygen resistance, as well as good flexibility and crack resistance. The density of the polysiloxane coating is 1.7 g/cm^3, which does not increase the weight of spacecraft and does not change the optical properties (transmittance and emissivity, etc.) of the substrate of the coating. Its anti-atomic oxygen property is apparently superior to some inorganic atomic oxygen resistance coatings commonly used in spacecraft, such as SiO_2, SiO_x and Al_2O_3, which is usually brittle and easily cracked [24–26,29,30]. Siloxane coating is generally prepared by a plasma polymerization deposition method. Its structure and properties are similar to that of SiO_x-PTFE, mainly including SiO_x as the main component for the atomic oxygen resistance and a small amount of C/H ingredients. Its structure and properties are similar to SiO_x-PTFE, containing a large amount of SiO_x and a small amount

of C/H components. Among them, SiO_x is used to protect atomic oxygen, and the C/H component is used to increase the flexibility of the coating, so compared with inorganic coating, the siloxane coating is not easy to crack [18].

This special component and structure configuration allow the siloxane coating to exhibit both excellent atomic oxygen resistance and good flexibility. The atomic oxygen resistance and lifetime of siloxane coating are both apparently superior to those of inorganic atomic oxygen barrier coatings [24–26]. The siloxane coating prepared by the plasma polymerization deposition technique has good uniformity on a large scale, which can be applied on the surface of a complex shape. Due to the compact structure, it is difficult for atomic oxygen to pass through the siloxane coating and erode the substrate materials, resulting in the longer service lifetime [31,32].

A siloxane coating is usually prepared by plasma polymerization deposition [33,34]. Plasma polymerization is a method of putting a reaction gas into a vacuum device chamber, using plasma discharge to ionize and dissociate a monomer into active small molecules and then polymerization reaction to form polymeric film. Plasma polymerization has some advantages over other vacuum coating methods. For example, it is easy to be operated and its operational parameters may be adjusted. The polymeric membrane prepared by this method has different chemical composition and physical properties from the ordinary polymeric membrane. Therefore, it is an effective new way to develop functional films and a new method to prepare new organic–inorganic hybrid coatings. The plasma polymerization device is similar to plasma chemical vapor deposition (PECVD), except that the gas used for discharge (working medium) is a polymerizable monomer and that the resulting coating contains organic components. There are some unique advantages to preparing coatings from a variety of organic and organometallic starting materials [35].

The thickness has a crucial influence on the atomic oxygen resistance and service lifetime of siloxane coating. For optimizing the design and development of the siloxane coating, therefore, it is very important and necessary to investigate the effect of thickness on the atomic oxygen resistance of siloxane coating and the underlying mechanism for atomic oxygen attacking the coating materials.

The effect of thickness on the atomic oxygen resistance of siloxane coatings was systematically studied in this article. A possible mechanism was proposed to explicate the physicochemical process of atomic oxygen attacking the coating materials.

2. Experimental Procedure

2.1. Synthesis of the Siloxane Coating

The siloxane coatings were prepared on the substrates by a self-developed plasma polymerization experimental device, which is a roll-to-roll plasma-enhanced chemical vapor deposition (PECVD) system with a 13.56 MHz radio frequency power supply. The working principle of a PECVD system is shown in the Figure 1. The discharge gas consisted of monomer hexamethyldisiloxane (HMDSO) and working gas (O_2), which both discharge in the coating vacuum chamber, and siloxane coating is deposited on the substrates on the winding shaft. The uniformity of the coating is maintained through the uniform rolling of the winding shaft. The ratio of oxygen to monomer was controlled by a gas flow controller, and the pressure in the discharge chamber was controlled by a butterfly valve.

The deposition rate of plasma polymerization is relatively complicated, which is related to the power of the deposition, the deposition pressure of discharge, the distance between two discharge plates, the partial pressure of oxygen and the transport rate of hexamethyldisiloxane. The thickness of a coating prepared in vacuum is generally controlled by deposition time and deposition power, and the thickness is strictly inversely proportional to the winding speed. In this experiment, based on the optimization of the main deposition parameters (deposition power, deposition pressure, monomer partial pressure), the coating thickness is mainly controlled by controlling the winding speed. The siloxane coatings were prepared respectively on the glass slides, Kapton and Kapton/Al substrates.

The glass slides, Kapton and Kapton/Al materials with a size of 25 mm × 75 mm × 25 μm, were selected as the different substrates.
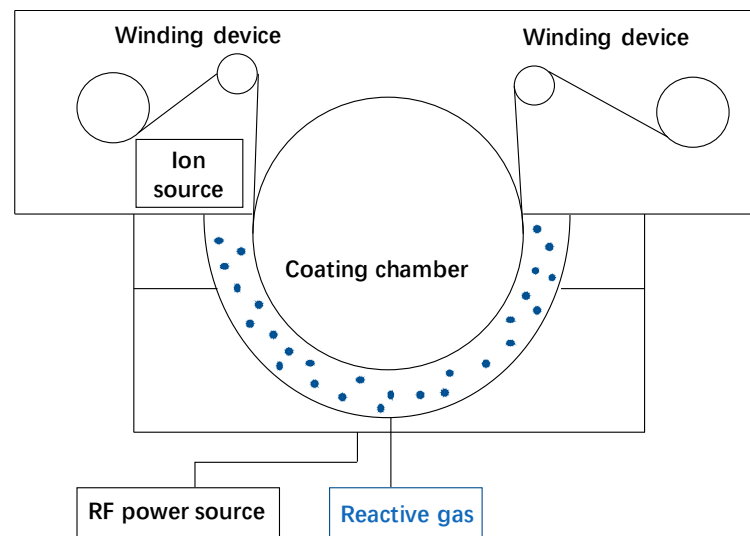
Figure 1. The working principle of a PECVD system.

The samples were cleaned before coating. Acetone can be used as a cleaning agent to clean difficult organic reagents. Alcohol is a very good solvent and is non-corrosive and can dissolve many inorganic, as well as organic, matter. It is also volatile, has no residue after use and has little effect on the coating substrates. Therefore, the substrate was first cleaned with acetone and then with alcohol in the experiment. In a typical run, the substrate material was ultrasonically cleaned in acetone for 5 min, then cleaned in alcohol for 10 min.

After drying in air, the substrate was adhered to the winding strip of the arc electrode plates. The distance between the plates was set to 15 cm, and the winding speed to 150 mm/min, then the chamber was evacuated to 5.0×10^{-3} Pa. Then Ar gas filled the chamber to clean the substrates with Ar plasma and activate the surface of the substrate, so as to increase the adhesion of coatings on the substrates. A certain proportion of the mixture of hexamethyldisiloxane monomer and O_2 was introduced into the chamber, and then the radio frequency source with a power of 400 W was turned on. Finally, the siloxane coatings with different thicknesses were obtained by setting different winding speeds.

2.2. Characteristics of the Silicone Coating

The coating thickness is very important to our research. Two methods were adopted to measure the film thickness: the mass method and the SEM method of testing a cross-section. The mass method is to weigh the substrate before and after the preparation of the coating and then to divide the increased weight by the density of the coating 1.7 g/cm^3 to obtain the volume of the coating, then divide the area of the substrate deposition surface to calculate the thickness of the coating. The SEM method of testing a cross-section is breaking the substrate after coating and obtaining a clear interface of the coating, then observing by SEM to measure the thickness of the coating.

In order to investigate the properties of various coatings, samples of different thicknesses were prepared. The thickness of a siloxane coating is controlled by using different winding speeds. The surface morphology and cross-section microstructure of siloxane coatings were observed by scanning electron microscopy (SEM, S-4800, Hitachi, Japan). An optical microscope model LV50 produced by Nikon was used to observe the surface morphology by taking optical micrographs with magnification of 200 times. The adhesion of a coating on the substrates was measured by pull-off testing using a 3 M tape (its nominal stripping strength is 0.47 N/mm); The reference standard of the damp-heat experiment is GB/T 2423.50-2012 Environmental testing-Part 2: Test methods-Test Cy: Damp heat, steady

state, accelerated test primarily intended for components. The duration of the damp-heat test was set at 60 days based on the satellite operating conditions document set by the customer. Cyclic damp-heat tests were carried out for 60 days by using a constant-temperature and -humidity chamber, and then the adhesion of coating on the substrates after the cyclic damp-heat tests was also measured.

The atomic oxygen resistance of a siloxane coating was measured by self-developed microwave source atomic oxygen ground simulation equipment. It generates microwave energy with a frequency of 2.45 GHz and an adjustable power of 150~1500 W from a microwave power source, which is coupled to the discharge room through a set of transmission system. The degree of vacuum of a discharge chamber is maintained at the order of 10^{-1} Pa. High-density plasma with 10^{12}~10^{13} atoms/cm^3 ions can be formed in the discharge chamber under the action of the magnetic field simultaneously. A neutral plate is negatively biased relative to the plasma to accelerate the oxygen ions in the plasma and make them obtain directional energy. Oxygen ions collide with a metal neutral plate with negative bias, from which they gain electrons and recombine to form neutral oxygen atoms. The reflected oxygen atoms retain most of the collision energy and form a neutral atomic oxygen beam with a certain amount of directional energy, which acts on the sample surface. By adjusting the bias of the neutral plate and changing the collision angle of the oxygen ions, the energy of the neutral atomic oxygen and the angular distribution after reflection can be adjusted. Since charged particles cannot cross magnetic field lines to the sample, the neutral atomic oxygen beam does not contain oxygen ions and electrons. The discharge chamber size is Ø100 cm × 100 cm, and the atomic oxygen flux is 10^{18}~10^{20} atoms/m^2/s. The test reference standard of the atomic oxygen experiment is QJ 20285-2014 Test method of atomic oxygen effect for spacecraft materials. The atomic oxygen energy generated by the equipment is in accordance with the real space-flight measurement in LEO space. Kapton is used as a calibration sample.

In the self-developed microwave source atomic oxygen ground simulation equipment, the content of molecular oxygen that can reach the sample surface is lower due to the restraint of the magnetic field, and the molecular oxygen is not accelerated by the electric field, so its energy is low. Similar to atmospheric environment of molecular oxygen, it cannot directly damage the sample.

The test parameters of atomic oxygen were set as follow: the background vacuum is 5×10^{-3} Pa; the microwave power source frequency is 2.45 GHz; the atomic oxygen energy is in the range from 5 eV to 8 eV; the the atomic oxygen flux is 1.0×10^{24} atoms/m^2/s, and the cumulative atomic oxygen flux is 2.5×10^{26} atoms/m^2.

The atomic oxygen resistance of the coatings is characterized by the atomic oxygen erosion yield, which is the volume change caused by each atomic oxygen impinging on the surface of materials. The atomic oxygen erosion yield was calculated according to Equation (1).

$$E_y = \frac{G_0 - G_1}{FA\rho} \tag{1}$$

where E_y is the atomic oxygen erosion yield (cm^3/atom), G_0 is the initial mass of the sample (g), G_1 is the mass after the test (g), A is the exposed surface area of the testing sample (m^2), ρ is the material density (g/cm^3), and F is cumulative atomic oxygen flux ($F = \Phi \cdot \tau$, atoms/m^2).

3. Results and Discussion

3.1. Thickness and Uniformity of the Silicone Coating

In order to investigate the thickness uniformity of the deposited large-area coating, 8 samples were prepared for each preparing conditions (winding speed). During the preparing process, 8 glass slides were placed in the effective coating range, and the position distribution of the slide samples is shown in Figure 2. The area of effective coating range is 85 mm × 240 mm.
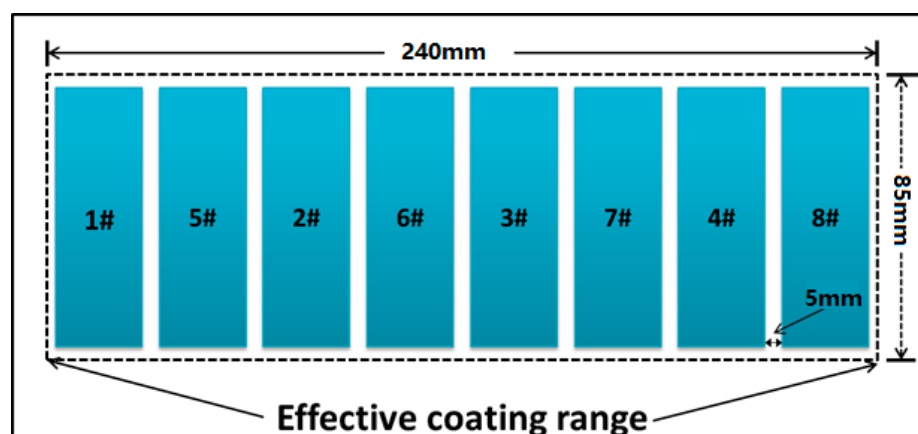
Figure 2. Position distribution of the glass slides on the sample holder.

The thickness of the siloxane coating was tested by the mass method, which is needed to weigh the increased weight of the sample after coating and then calculate the thickness of the coating according to the coating density and the coating surface area. In the experiment, four samples were selected for thickness testing with the mass method. After the coating process was completed, the masses of the glass-slide samples were weighed. The density of the siloxane coating was 1.7 g/cm^3. For example, when the winding speed was 29 mm/min, the thickness results measured by the mass method ($H = \Delta M / \rho S$) were 387.5 nm, 368.9 nm, 368.9 nm and 370.7 nm, and the average value was about 374 nm. The thickness uniformity of the siloxane coating prepared by plasma polymerization, is mainly related to the distribution of the reactive gas. The coating uniformity can be controlled by controlling the flow and distribution of the reactive gas.

Then, a series of coatings were prepared with different winding speeds, and the thickness of the coating samples is shown in Table 1.

Table 1. Average thickness of the siloxane coatings prepared with different winding speeds.

Winding Speed (mm/min)	Average Thickness of Coatings (nm)
54	198
32	335
30	360
29	374
26	418
21	510
17	615

3.2. Morphologies of the Siloxane Coating

The surface/section morphologies of the siloxane coatings observed by SEM are shown in Figure 3. The surface of the 335 nm-thick coating has many round protrusions (shown in Figure 3a), while other samples with thickness of 360 nm, 374 nm and 418 nm have relatively flat, uniform and dense surfaces (shown in Figure 3b–d). These SEM results validate the reliability of the coating thickness data measured by the mass method.

The sample with thickness of 418 nm in Figure 3d was observed by magnifying 200 times with an optical microscope, as shown in Figure 4. Scanning electron microscopy was used to observe the surface microstructure of the same sample, as shown in Figure 5. The surface was uniform and dense, without obvious defects such as bumps and pits. The porosity of the coating was not tested or simulated in this paper.
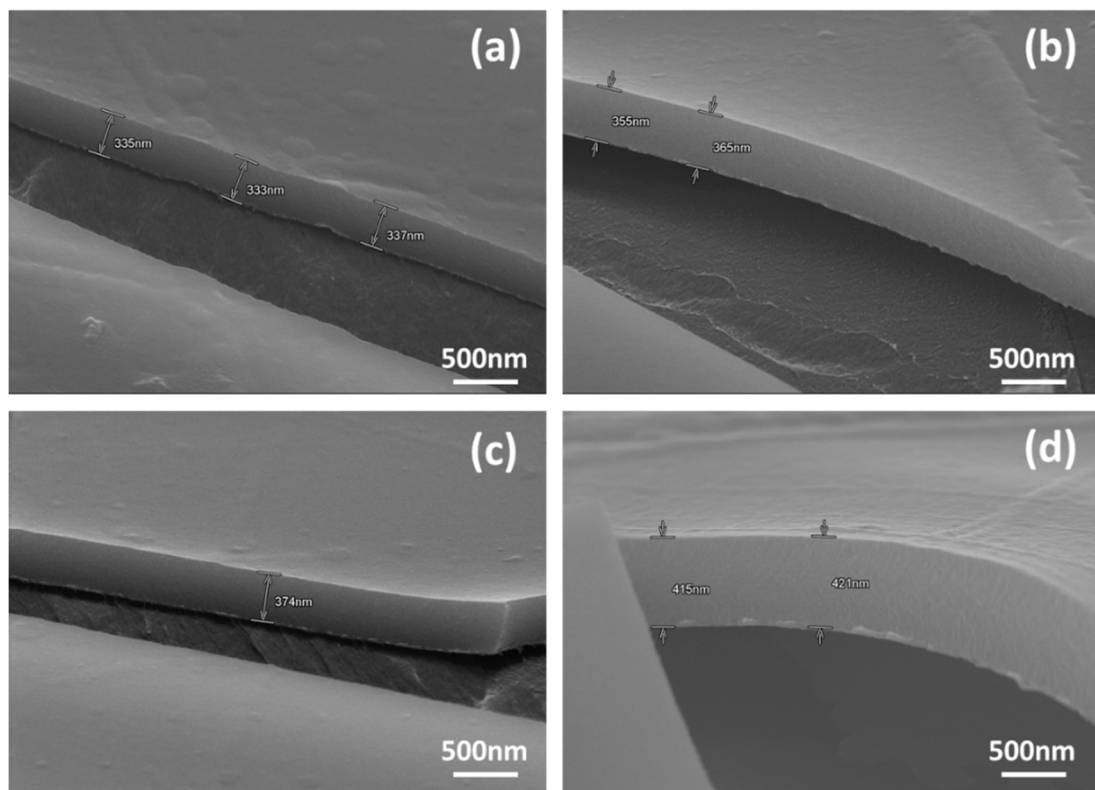
Figure 3. Surface/section morphologies of the siloxane coatings with different thicknesses. (**a**) 335 nm; (**b**) 360 nm; (**c**) 374 nm and (**d**) 418 nm.
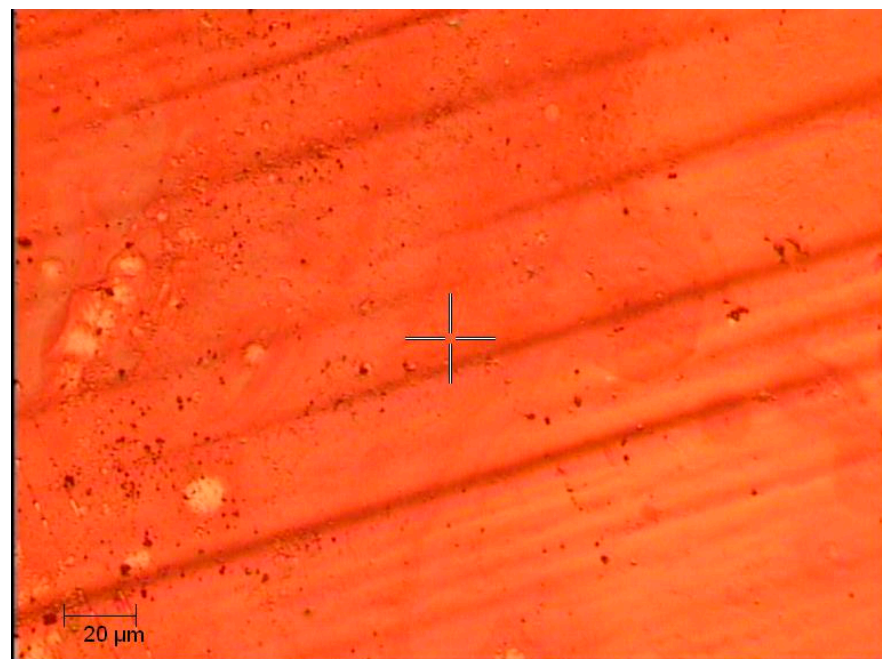
Figure 4. Photomicrograph of the sample with thickness of 418 nm at $200\times$ magnification.
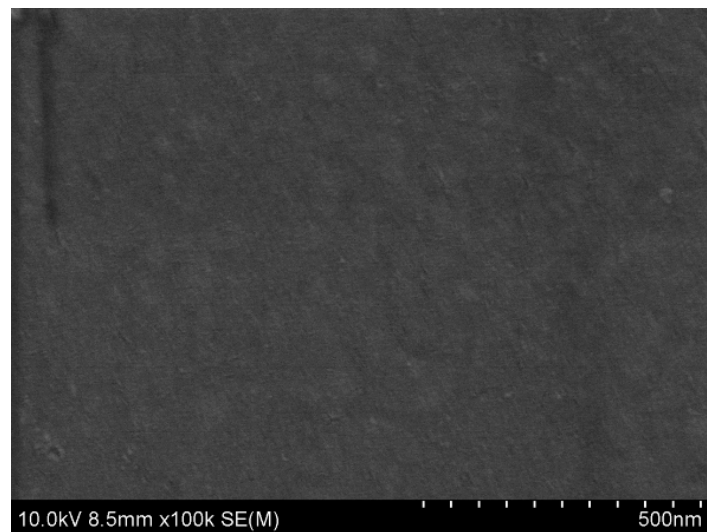
Figure 5. SEM surface morphology photos of the sample with thickness of 418 nm in Figure 3d.

3.3. Cyclic Damp-Heat Test for the Siloxane Coating

The siloxane coating samples with the thickness of 374 nm, 418 nm and 615 nm were subjected to the cyclic damp-heat test of 60 days with a humidity of 70% RH (relative humidity) at a temperature of 30 °C. The adhesion test was carried out by sticking a 3 M tape (product number 898#) after the cyclic damp-heat test. Microscopic surface topography analysis was performed on the samples before and after the test. The surface topographies of the samples with the thickness of 374 nm and 418 nm are shown in Figure 6. No obvious peeling and cracking of the coatings were observed after the cyclic damp-heat testing, indicating that the coatings with the thickness of 374 nm and 418 nm showed good wet-heat resistance.
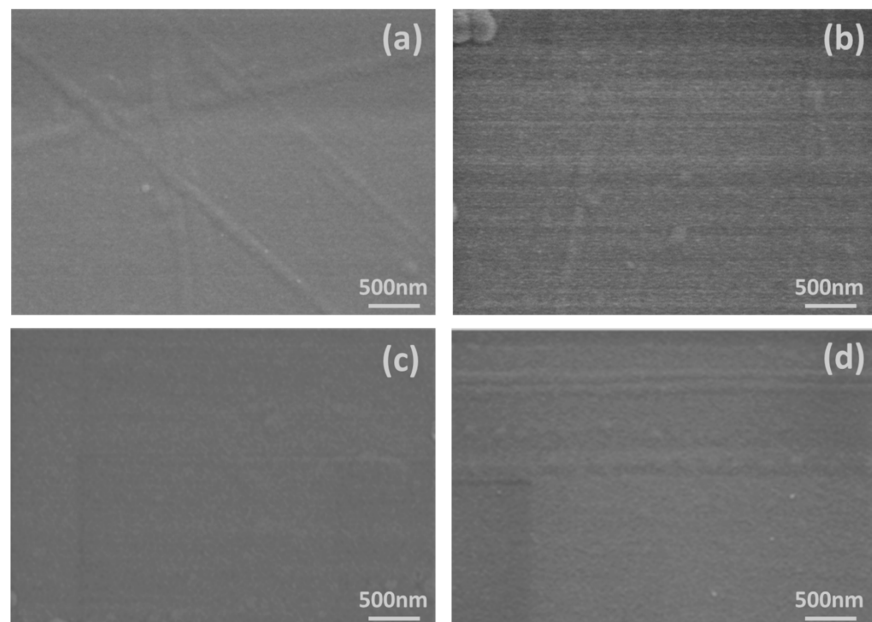
Figure 6. Surface topographies of siloxane coating (**a**,**c**) before the damp-heat test and (**b**,**d**) after the damp-heat test and adhesion test. (**a**,**b**) The 374 nm-thick the siloxane coating; (**c**,**d**) the 418 nm-thick siloxane coating.

The surface topography of the coating with the thickness of 615 nm after the damp-heat test and adhesion test is shown in Figure 7. Although no obvious peeling of the coatings was observed, apparent micro-cracks were observed on the coating. This results

indicate that coatings with thick thickness may be prone to the cracking of the siloxane coating due to the larger cyclic internal stresses near the coating/substrate interface during damp-heat testing.
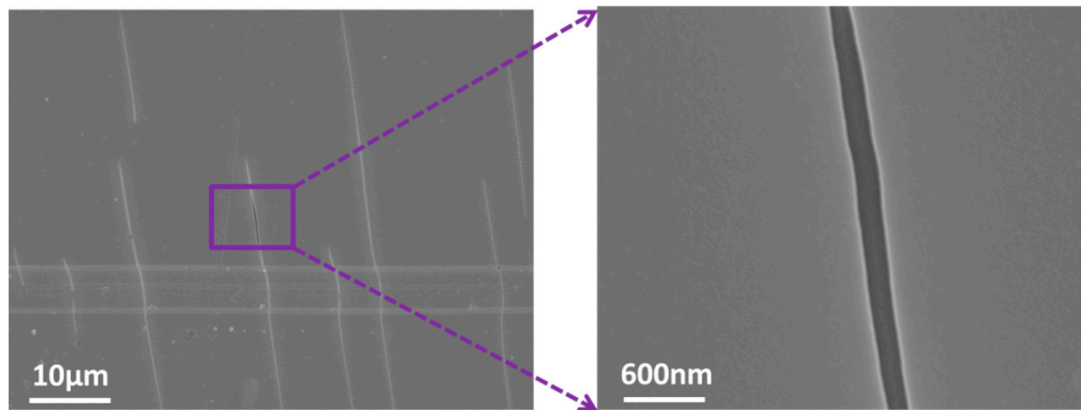
Figure 7. Surface topography of the siloxane coating with the thickness of 615 nm after the damp-heat test and adhesion test.

3.4. Atomic Oxygen Resistance of the Siloxane Coating

The atomic oxygen resistance test was carried out on the siloxane-coated samples with the Kapton/Al substrate. For comparison, two samples were selected for the test. Sample (a) was the uncoated sample of the Kapton/Al substrate, and sample (b) was the siloxane-coated sample with the Kapton/Al substrate. The thickness of the siloxane coating of sample (b) was 360 nm. The cumulative atomic oxygen flux was 2.5×10^{26} atoms/m^2. This was designed to simulate a 5-year flight of spacecraft in LEO space. The uncoated and coated samples were taken out after the atomic oxygen irradiation test. As shown in Figure 8a, the uncoated sample (a) was completely destroyed. The 25 μm-thick Kapton was completely eroded, and the Al film substrate was broken. However, as shown in Figure 8b, the siloxane-coated sample (b) presented a good and smooth appearance, and no obvious eroded or broken morphology was visually observed. This indicates that the siloxane coating indeed exhibits excellent atomic oxygen resistance.
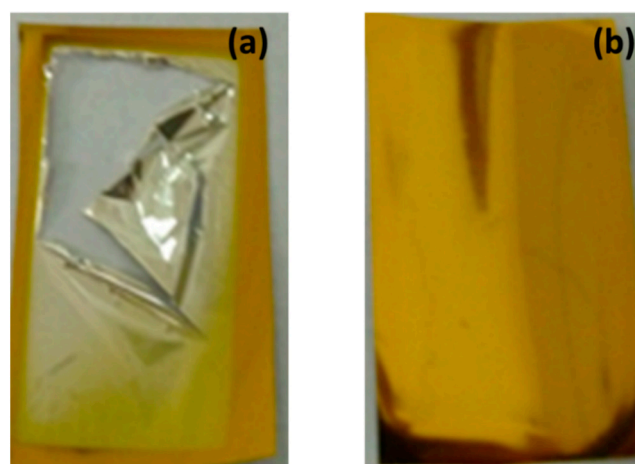
Figure 8. Images of the Kapton/Al samples (**a**) uncoated and (**b**) with the 360 nm-thick siloxane coating after the atomic oxygen irradiation test.

The atomic oxygen protection properties of samples with different thicknesses vary greatly. In order to compare the effects of different thicknesses on the corrosion characterization, different winding speeds were used to prepare samples of different thicknesses.

Samples with different thicknesses were selected for characterization. Samples were prepared in turn from fast winding speed to slow winding speed.

In order to accurately characterize the atomic oxygen resistance, the siloxane coating samples with different thicknesses were subjected to an atomic oxygen irradiation test with a cumulative atomic oxygen flux of 2.5×10^{26} atoms/m^2. The mass changes of the samples were accurately recorded before and after the atomic oxygen irradiation test, which are used to calculate the atomic oxygen erosion yield of the coatings on the basis of Equation (1). In order to clearly express the influence of coating thickness on the atomic oxygen resistance of a siloxane coating, the relationship between the atomic oxygen erosion yield E_y and the coating thickness H was plotted in Figure 9. Firstly, all the samples were in good appearance after 2.5×10^{26} atoms/m^2 of atomic oxygen, and no obvious eroded or broken morphology was visually observed. Based on the results shown in Figure 9, it can be deduced that the coatings with a thickness between 300 nm and 500 nm exhibit relatively low erosion yield. In particular, coatings with a thickness of around 400 nm exhibit the best atomic oxygen resistance. The atomic oxygen erosion yield of a 418 nm-thick siloxane coating is as low as 5.39×10^{-27} cm^3/atoms, which is decreased by about three orders of magnitude compared to that of the uncoated Kapton substrate ($E_y \approx 3.0 \times 10^{-24}$ cm^3/atoms).
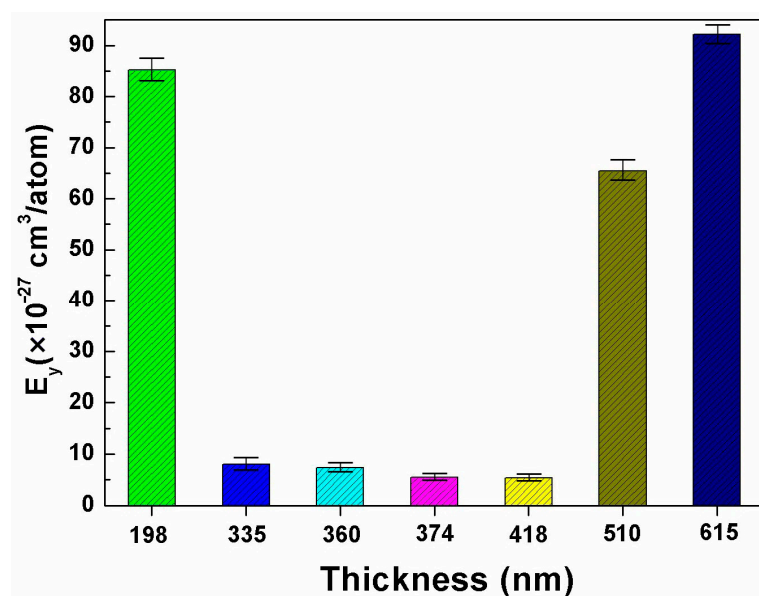
Figure 9. Relationship between the atomic oxygen erosion yield and the coating thickness.

3.5. Mechanism of the Atomic Oxygen Attacking Materials

Based on the above results and analysis, when the thickness is lower than 200 nm, siloxane coatings present a poor atomic oxygen resistance, since the thin coatings are insufficient to resist the erosion of larger atomic oxygen fluxes. In the meantime, when the coating thickness is higher than 500 nm, siloxane coatings also present poor atomic oxygen resistance, probably due to the existence of abundant defects or micro-cracks in the thicker coating and the larger internal stresses. As shown in Figure 7, the apparent micro-cracks were observed in the coating with a thickness of 615 nm after a long damp-heat test of 60 days. These micro-cracks are prone to occur after the damp-heat test because there are large internal stresses in the thicker coating. The thermal effects caused by the large flux of atomic oxygen bombardment on the surface of the coating are similar to the damp-heat test.

On basis of the above analysis, a possible mechanism of the atomic oxygen attacking materials was proposed herein. As shown in Figure 10, the siloxane coating is graphically represented by orthogonal array cells. Each cell denotes a group of siloxane atoms that can possibly be eroded by an atomic oxygen group. Concerning the surface of a coating without crack defects (Figure 10a), two physicochemical processes will occur when the high-energy atomic oxygen groups bombard the surface of coatings: (1) One coating cell

can be completely etched by the atomic oxygen group; (2) when the energy of the atomic oxygen group is not high enough to erode the coating cell, it will be scattered back into the space. In the meantime, the atomic oxygen group bombarding the coating surface will generate a thermal effect to heat the coating materials. Conversely, a very different process can occur in coating materials with a large number of micro-cracks on the surface. As shown in Figure 10b, when the surface of a coating has defects such as cracks or holes, the atomic oxygen group will enter into the defects from the surface. Then, the atomic oxygen group will oscillate back and forth inside the defects until their energy is exhausted. The above two physicochemical processes occur each time an atomic oxygen collides with the coating materials. It means that an atomic oxygen group interacts multiple times with the coating materials, which will greatly accelerate the erosion process of the coatings. In particular, the thermal effect caused by atomic oxygen bombardment in the second physicochemical process will produce more micro-cracks inside the coating material due to the thermal effect, which will further accelerate the damage to the coating. These two physicochemical processes result in the undercutting effect of atomic oxygen [36–39]. At a certain extent, the size of the cracks or holes formed by the undercutting effect of atomic oxygen may be much larger than the original size of the defects on the surface of the coating. This process will result in coating failure and thereby cause destructive damage to the substrate material. Therefore, it is very important and necessary to select an optimum thickness during the preparation of the siloxane coating so as to obtain excellent atomic oxygen resistance.
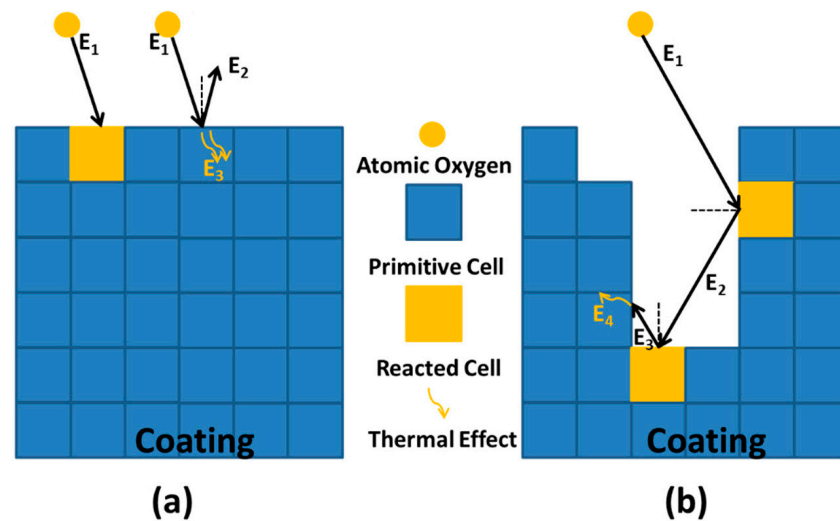
Figure 10. Schematics for mechanism of the atomic oxygen attacking the siloxane coating materials (**a**) without cracks and (**b**) with cracks.

4. Conclusions

Siloxane coatings with different thicknesses were prepared with the plasma polymerization deposition technique and evaluated by atomic oxygen resistance testing. The results showed that the coating thickness plays an important role on the atomic oxygen resistance of silicone coatings. When the coating thickness is below 200 nm, siloxane coatings present poor atomic oxygen resistance. As the coating thickness reaches about 400 nm, the atomic oxygen resistance of siloxane coating is optimal. After an atomic oxygen irradiation test with a cumulative atomic oxygen flux of 2.5×10^{26} atoms/m^2, the atomic oxygen erosion yield of a 418 nm-thick siloxane coating is as low as 5.39×10^{-27} cm^3/atoms, which is decreased by about three orders of magnitude compared to that of the uncoated Kapton substrate. When the coating thicknesses are greater than 500 nm, the atomic oxygen erosion yield increases with the increase in the coating thickness. It should be ascribed to the existence of abundant micro-cracks or holes inside the thicker coatings caused by the large internal stress. Consequently, the undercutting effect of atomic oxygen occurred inside

these cracks accelerates the erosion process of coating materials and causes the sudden increase in erosion yield. Overall, the siloxane coating with a thickness of about 400 nm has an optimal atomic oxygen resistance and comprehensive physical properties. It is believed that the results and analysis presented in this paper will be very useful for optimizing the design and development of siloxane coatings to improve atomic oxygen resistance.

Author Contributions: Conceptualization, L.Z. and H.C.; methodology, L.Z. and Z.C.; formal analysis, L.Z. and B.B.; investigation, L.Z. and H.C.; data curation, L.Z. and R.Z.; writing—original draft preparation, L.Z., J.H. and H.C.; writing—review and editing, L.Z. and H.C.; supervision, X.L. and H.C.; funding acquisition, X.L., J.L. and H.C. All authors have read and agreed to the published version of the manuscript.

Institutional Review Board Statement: Not applicable.

Informed Consent Statement: Not applicable.

Data Availability Statement: The data presented in this study are available on request from the corresponding author.

Conflicts of Interest: The authors declare no conflict of interest.

References

1. Dignam, A.; Wozniakiewicz, P.J.; Burchell, M.J.; Alesbrook, L.S.; Tighe, A.; Suliga, A.; Wessing, J.; Kearsley, A.; Bridges, J.; Holt, J.; et al. Palladium-coated kapton for use on dust detectors in low earth orbit: Performance under hypervelocity impact and atomic oxygen exposure. *Front. Space Technol.* **2022**, *3*, 933664. [CrossRef]
2. Jiang, H.; Jiang, L.; Li, T.; Zheng, H.; Liu, P.; Yang, Q.; Yuan, X.; Yang, D.; Zang, W.; Wang, L. Current situation and development trend of neutral atmosphere simulation test technology. *Spacecr. Environ. Eng.* **2022**, *39*, 460–467. (In Chinese) [CrossRef]
3. De Groh, K.K.; Banks, B.A. *Atomic Oxygen Erosion Data from the MISSE 2–8 Missions*; Technology Report; NASA/TM—2019-219982; National Aeronautics and Space Administration Glenn Research Center: Cleveland, OH, USA, 2019.
4. Silverman, E.M. *Space Environmental Effects on Spacecraft: LEO Materials Selection Guide: II. Progress Report*; Technology Report; CR-4661; NASA Langley Technical Report: Langley, BC, Canada, 1995.
5. Whiteside, J.B.; Kamykowski, E.; Rooney, W.D.; Schulte, R.; Stauber, M. Effects of 69 months in low Earth orbit on Kapton antenna structures. *J. Spacecr. Rocket.* **1994**, *31*, 860–865. [CrossRef]
6. Shimamura, H.; Nakamura, T. Investigation of degradation mechanisms in mechanical properties of polyimide films exposed to a low earth orbit environment. *Polym. Degrad. Stab.* **2010**, *95*, 21–33. [CrossRef]
7. Gregory, J.C.; Peters, P.N. The reactions of 5 eV oxygen atoms with polymeric and carbon surfaces in orbit. *Polymer* **1987**, *28*, 459–460.
8. Zimcik, D.G.; Maag, C.R. Results of apparent atomic oxygen reactions with spacecraft materials during Shuttle flight STS-41G. *J. Spacecr. Rocket.* **1988**, *25*, 162–168. [CrossRef]
9. Reddy, M.R. Effect of low earth orbit atomic oxygen on spacecraft materials. *J. Mater. Sci.* **1995**, *30*, 281–307. [CrossRef]
10. Banks, B.A.; Miller, S.K.; de Groh, K.K. Low Earth Orbital Atomic Oxygen Interactions with Materials. In Proceedings of the 2nd International Energy Conversion Engineering Conference, Providence, RI, USA, 16–19 August 2004.
11. Ma, A.; Huang, X. Development of Manned Space Environmental Simulation Technology. *Space Med. Med. Eng.* **2008**, *21*, 224–232. (In Chinese) [CrossRef]
12. Arnold, G.S.; Peplinski, D.R. Reaction of atomic oxygen with polyimide films. *AIAA J.* **1985**, *23*, 1621–1626. [CrossRef]
13. Koontz, S.L.; Albyn, K.; Leger, L.J. Atomic oxygen testing with thermal atom systems—A critical evaluation. *J. Spacecr. Rocket.* **1991**, *28*, 315–323. [CrossRef]
14. Duo, S.; Meishuan, L.I.; Zhang, Y.; Yan, C. Atomic oxygen attack on space materials in LEO environment and protective coatings. *Corros. Sci. Technol. Prot.* **2022**, *14*, 152–156.
15. Xiong, Y.Q.; Xie, S.P. Measurement methods of atomic oxygen concentration. *J. Transducer Technol.* **1999**, *18*, 8–12.
16. Semonin, D.L.; Brunsvold, A.M.; Minton, T.K. Erosion of Kapton H® by hyperthermal atomic oxygen. *J. Spacecr. Rocket.* **2006**, *43*, 421–425.
17. Banks, B.; Rutledge, S.; Stueber, T.; Snyder, S.; Norris, M.; Norris, M. *Atomic Oxygen Erosion Phenomena*; AIAA-97-3903; American Institute of Aeronautics and Astronautics: Reston VA, USA, 1997.

18.　Hu, L.; Li, M.; Zhou, Y. Effects of Vacuum Ultraviolet Radiation on Atomic Oxygen Erosion of Polysiloxane/SiO2 Hybrid Coatings. *J. Mater. Sci. Technol.* **2009**, *25*, 483–488.

19.　Tagawa, M.; Yokota, K. Atomic oxygen-induced polymer degradation phenomena in simulated LEO space environments: How do polymers react in a complicated space environment? *Acta Astronaut.* **2008**, *62*, 203–211. [CrossRef]

20.　Minton, T.K.; Wright, M.E.; Tomczak, S.J.; Marquez, S.A.; Shen, L.H.; Brunsvold, A.L.; Cooper, R.; Zhang, J.M.; Vij, V.; Guenthner, A.J.; et al. Atomic Oxygen Effects on POSS Polyimides in Low Earth Orbit. *ACS Appl. Mater. Interfaces* **2012**, *4*, 492–502. [CrossRef] [PubMed]

21.　Hu, L.; Li, M.; Xu, C.; Luo, Y.; Zhou, Y. A polysilazane coating protecting polyimide from atomic oxygen and vacuum ultraviolet radiation erosion. *Surf. Coat. Technol.* **2009**, *203*, 3338–3343. [CrossRef]

22.　Wu, W.; Lv, H.; Wang, D.; Du, L. Protection of Kapton from atomic-oxygen erosion using alumina film deposited by magnetron sputtering. In Proceedings of the MATEC Web of Conferences; EDP Sciences: Les Ulis, France, 2016; Volume 67, p. 04023.

23.　Qi, H.; Qian, Y.; Xu, J.; Li, M. Studies on atomic oxygen erosion resistance of deposited Mg-alloy coating on Kapton. *Corros. Sci.* **2017**, *124*, 56–62. [CrossRef]

24.　Banks, B.A.; Rutledge, S.K.; De Groh, K.K.; Auer, B.M.; Mirtich, M.J.; Gebauer, L.; Hill, C.M.; Lebed, R.F. LDEF spacecraft ground laboratory and computational modeling implications on Space Station Freedom's solar array materials and surfaces durability. In Proceedings of the IEEE Photovoltaic Specialists Conference, Las Vegas, NV, USA, 7–11 October 1991; Volume 2, pp. 1434–1439.

25.　Banks, B.; Rutledge, S.; Gebauer, L.; LaMoreaux, C. SiO(X) coatings for atomic oxygen protection of polyimide Kapton in low earth orbit. In Proceedings of the Materials Specialist Conference-Coating Technology for Aerospace Systems, Dallas, TX, USA, 16–17 April 1992.

26.　Banks, B.A.; Rutledge, S.K.; Cales, M. Performance characterizations of EURECA Retroreflectors with fluoropolymer-filled SiOx protective coatings. In *Proceedings of the NASA. Langley Research Center, LDEF: 69 Months in Space. Third Post-Retrieval Symposium*; NASA: Washington, DC, USA, 1995.

27.　Miyazaki, E.; Tagawa, M.; Yokota, K.; Yokota, R.; Kimoto, Y.; Ishizawa, J. Investigation into tolerance of polysiloxane-block-polyimide film against atomic oxygen. *Acta Astronaut.* **2010**, *66*, 922–928. [CrossRef]

28.　Lei, X.; Qiao, M.; Tian, L.; Chen, Y.; Zhang, Q. Evolution of surface chemistry and morphology of hyperbranched polysiloxane polyimides in simulated atomic oxygen environment. *Corros. Sci.* **2015**, *98*, 560–572. [CrossRef]

29.　Cooper, R.; Upadhyaya, H.P.; Minton, T.K.; Berman, M.R.; Du, X.; George, S.M. Protection of polymer from atomic-oxygen erosion using Al2O3 atomic layer deposition coatings. *Thin Solid Films* **2008**, *516*, 4036–4039. [CrossRef]

30.　Liu, K.; Mu, H.; Shu, M.; Li, Z.; Gao, Y. Improved adhesion between SnO2/SiO2 coating and polyimide film and its applications to atomic oxygen protection. *Colloids Surf. A Physicochem. Eng. Asp.* **2017**, *529*, 356–362. [CrossRef]

31.　Song, G.; Li, X.; Jiang, Q.; Mu, J.; Jiang, Z. A novel structural polyimide material with synergistic phosphorus and POSS for atomic oxygen resistance. *RSC Adv.* **2015**, *5*, 11980–11988. [CrossRef]

32.　Vernigorov, K.B.; Alentev, A.Y.; Meshkov, I.B. Use of Hyper-branched Polyethoxysiloxane to Improve the Resistance of Thermo-plastic Polyimide Coatings to Atomic Oxygen Environment. *Inorg. Mater. Appl. Res.* **2012**, *3*, 81–87. [CrossRef]

33.　Zheng, K.; Yang, S.; Li, Z.; Wang, J.; Zhao, L. The preparation of organic silicon atomic-oxygen-protection film and its properties. *Spacecr. Environ. Eng.* **2010**, *6*, 751–755. (In Chinese) [CrossRef]

34.　Angelini, E.; D'Agostino, R.; Fracassi, F.; Grassini, S.; Rosalbino, F. Surface analysis of PECVD organosilicon films for corrosion protection of steel substrates. *Surf. Interface Anal.* **2002**, *34*, 155–159. [CrossRef]

35.　Mu, H.; Wang, X.; Li, Z.; Xie, Y.; Gao, Y.; Liu, H. Preparation and atomic oxygen erosion resistance of SiOx coating formed on polyimide film by plasma polymer deposition. *Vacuum* **2019**, *165*, 7–11. [CrossRef]

36.　Yokota, K.; Tagawa, M.; Ohmae, N. Temperature Dependence in Erosion Rates of Polyimide Under Hyperthermal Atomic Oxygen Exposures. *J. Spacecr. Rocket.* **2003**, *40*, 143–144. [CrossRef]

37.　de Groh, K.K.; Banks, B.A. Atomic-oxygen undercutting of long duration exposure facility atomized-Kapton multilayer insulation. *J. Spacecr. Rocket.* **1994**, *31*, 656–664. [CrossRef]

38.　Banks, B.A.; Snyder, A.; Miller, S.K.; De Groh, K.K.; Demko, R. Atomic-Oxygen Undercutting of Protected Polymers in Low Earth Orbit. *J. Spacecr. Rocket.* **2004**, *41*, 335–339. [CrossRef]

39.　Liu, Y.; Li, G. Numerical simulation on atomic oxygen undercutting of Kapton film in low earth orbit. *Acta Astronaut.* **2010**, *67*, 388–395. [CrossRef]